Analysis of the non-Markov parameter in continuous-time signal processing

J. J. Varghese,* P. A. Bellette, K. J. Weegink, A. P. Bradley, and P. A. Meehan
University of Queensland, Brisbane, Australia
(Received 16 September 2013; published 10 February 2014)

The use of statistical complexity metrics has yielded a number of successful methodologies to differentiate and identify signals from complex systems where the underlying dynamics cannot be calculated. The Mori-Zwanzig framework from statistical mechanics forms the basis for the generalized non-Markov parameter (NMP). The NMP has been used to successfully analyze signals in a diverse set of complex systems. In this paper we show that the Mori-Zwanzig framework masks an elegantly simple closed form of the first NMP, which, for C^1 smooth autocorrelation functions, is solely a function of the second moment (spread) and amplitude envelope of the measured power spectrum. We then show that the higher-order NMPs can be constructed in closed form in a modular fashion from the lower-order NMPs. These results provide an alternative, signal processing-based perspective to analyze the NMP, which does not require an understanding of the Mori-Zwanzig generating equations. We analyze the parametric sensitivity of the zero-frequency value of the first NMP, which has been used as a metric to discriminate between states in complex systems. Specifically, we develop closed-form expressions for three instructive systems: band-limited white noise, the output of white noise input to an idealized all-pole filter, f and a simple harmonic oscillator driven by white noise. Analysis of these systems shows a primary sensitivity to the decay rate of the tail of the power spectrum.

DOI: 10.1103/PhysRevE.89.022109 PACS number(s): 05.40.−a, 87.85.Ng, 89.75.−k

I. INTRODUCTION

Time series analysis is often employed to characterize systems where the generating physics is either too complex or involves too many degrees of freedom to be predicted. These systems frequently arise in financial [1,2] and biological [3–6] systems. One of the earliest metrics used to characterize a system is the Shannon information entropy, which ascribes a numerical score to the system based on the randomness of the underlying statistics driving the process [7]. This methodology, originally used in communications theory, was adapted to nonlinear deterministic dynamical systems with the use of Kolmogorov-Sinai entropy [8]. While successful for the analysis of chaotic systems this approach can fail to detect the statistical simplicity of random behavior [9]. This has motivated the development of "statistical complexity metrics," which measure the correlation structure of an interacting system and its subsets [10], allowing for the analysis of multi degree of freedom probabilistic systems.

This methodology has generated a plethora of statistical complexity metrics, often with ambiguous relationships to each other, which often do not provide a clear interpretation of what the metric is actually measuring [10]. The application of these complexity metrics to time series analysis has thus seen the emergence of an interesting phenomenon where signals from complex systems can be successfully differentiated, but there is little insight into the nature of these differences.

An excellent example of this problem has been the application of the generalized non-Markov parameter (NMP), which is effectively a complexity metric developed from the Mori-Zwanzig theory of nonequilibrium statistical physics [11]. The NMP has been used in a diverse range of fields such as geology [12], astrophysics [13], cardiology [5], and neurophysiology [6]. In these complex systems the NMP has been developed as an informational tool to analyze the degree of randomness or "Markovity" of the system. Particular attention has been paid to the zero-frequency value of the first-order NMP (ZF-NMP_1) [5,12,14,15], which in a similar sense to the Shannon information entropy maps the Markovity of a system interacting with its environment to a scale from unity for non Markov processes (the transition to the next state is history dependent) to infinity for purely Markov processes (the transition to the next state is history independent) [11]. In specific applications the quantification of this randomness has proved useful as a metric of discrimination between different states in complex systems. More recently we have used the ZF-NMP_1 to differentiate states of microelectrode recordings of the subthalamic nucleus of patients with Parkinson's disease during linguistic processing tasks [16].

Previous papers have derived the NMP for measured systems from discrete time equations to define chaos or a non-Markov correlation structure between a system and its environment [11]. This paper will show that for stationary processes the NMP can be expressed in closed form in terms of operations on the power spectrum of the measured system. It is then shown that with the additional constraint of a smooth autocorrelation function (specifically belonging to the C^1 or higher differentiability class) the first NMP has a particularly simple structure depending solely on the spread and amplitude envelope of the measured power spectrum. These results provide a more conventional signal processing perspective from which to understand the NMP in terms of the power spectrum of the measured system. This result is entirely complementary to the original Mori-Zwanzig framework of complex interactions between the measured system and its environment. In essence these results allow the NMP to be expressed simply without a detailed understanding of Mori-Zwanzig theory.

We then go on to show that closed-form expressions for the higher-order NMP can be constructed in a modular fashion by a set of nonlinear operations on the measured power spectrum.

*john.varghese@uqconnect.edu.au

We then suggest, but do not prove, that these operations remove correlation structure from the spectrum and thus there is limited information about the system in the higher-order NMP. This analysis is consistent with Ref. [17], which argues the memory kernels can "veil" the properties of the physical system. The ZF-NMP$_1$ is then analytically calculated for three instructive systems: simple harmonic oscillator (SHO) driven by white noise, band-limited white noise, and white noise passed through an ideal all pole filter. We show that the dominant feature of ZF-NMP$_1$ is the slope of the tail of the measured power spectrum. We lastly show with numerical simulation that these expressions are also valid for noisy sampled systems where the power spectrum is not known *a priori*.

The work performed in this paper may be considered an extension to that in Ref. [18]. The work in Ref. [18] is concerned with developing the zero-frequency NMP for dynamical systems defined from time propagation operators with causal correlation functions. This greatly simplifies the spectral analysis (principally because the Fourier transforms (FT) can be represented as Laplace transforms rotated by 90°). This article, however, is concerned with deriving analytical expressions for the generalized NMP spectra for measured systems, that is, with autocorrelation functions defined for positive and negative lags. Last, this work is concerned with observing how the NMP varies with the measured power spectrum, whereas Ref. [18] uses successively higher-order zero-frequency values of the non-Markov parameters to explicitly explore the Markovity of specific causal systems.

This paper is organized as follows. Section II gives an overview of the Mori-Zwanzig kinetic equations from which the NMP is derived. Section III develops closed-form expressions for the hierarchy of generalized NMPs and shows how the zero-frequency value of the NMPs can be simplified. Section IV uses these simplifications to derive analytical expressions for the ZF-NMP$_1$ for three stochastic processes. The analysis of the SHO driven by white noise provides a conceptual bridge between the analysis of the Markovity of the physical system and the signal processing interpretation of the ZF-NMP$_1$ introduced in this paper. The analysis of the band-limited white noise and the ideal all-pole filter provide an explicit understanding of how this parameter varies with spectral properties of corner frequencies and stop band decay rates. Section V determines the generalized NMP from the discrete time series data of a model of the SHO driven by white noise. This highlights that the closed-form expressions for the generalized NMP are applicable to "real world" problems where only noisy sampled realizations of a process are available.

II. MORI-ZWANZIG KINETIC EQUATIONS

Consider a system of interacting objects with defined observables that completely describe the phase space of the system of interest. Often we are only concerned with the evolution of a subset of all the objects in the system. For example, the voltage contribution to an electrode of the closest neuron in a highly connected neural network.

The number of observables of interest can be extended to an arbitrarily high number but for simplification we will consider the evolution of one observable $\mathcal{G}(t)$. The evolution of the observable of interest is described by a generalized Langevin equation (GLE) [19]:

$$\dot{\mathcal{G}}(t) = \lambda_0 \mathcal{G}(t) - \Lambda_0 \int_0^t m_1(t-t')\mathcal{G}(t')dt' + \mathcal{S}(t) \quad t \geqslant 0, \tag{1}$$

where $\mathcal{G}(t)$ and $\dot{\mathcal{G}}(t)$ are the observable of interest and its time derivative, respectively, t' is a dummy variable of integration, $m_1(t)$ is the first memory kernel which introduces history dependence, $\mathcal{S}(t)$ is a stochastic forcing function, and λ_0 & Λ_0 are the zeroth-order relaxation parameters.

The contribution of the neglected variables is accounted for in the memory (convolution) function and stochastic forcing terms. The convolution term is a consequence of a general result that when the evolution of a multi-degree-of-freedom dynamic system, which is history independent, is described by a reduced number of degrees of freedom it is transformed to a history-dependent dynamical system [20]. The presence of the stochastic forcing term is a consequence of the state vector, which describes the observables of interest. This resides in a subspace of the Hilbert space of the full dynamic system at time zero, rotating as time increases outside of this subspace into the full Hilbert space. The evolution of this state vector outside this subspace is modeled as stochastic forces randomly rotating the state vector [20].

The difficulty with the GLE Eq. (1) is that the presence of the noise term makes the system a *stochastic* integrodifferential equation, which is mathematically difficult to analyze. The equation can be reduced to a standard integrodifferential by projecting the observable at time zero $\mathcal{G}(0)$ onto the evolution equation and performing an ensemble average $\langle \cdots \rangle$. The noise terms are constructed such that for all time they stay orthogonal to the observable at time zero [21], and thus the noise term is removed. Thus,

$$\langle \mathcal{S}(t)\mathcal{G}(0) \rangle = 0 \tag{2}$$

$$\langle \mathcal{G}(t)\mathcal{G}(0) \rangle = m_0(t), \tag{3}$$

where $m_0(t)$ is the autocorrelation function of the observable $\mathcal{G}(t)$. Applying these operations to Eq. (1) yields an integrodifferential equation for the evolution of the autocorrelation function, $m_0(t)$, of our single observable of interest [20]:

$$\frac{dm_0(t)}{dt} = \lambda_0 m_0(t) - \Lambda_0 \int_0^t m_1(t-t')m_0(t')dt' \quad t \geqslant 0. \tag{4}$$

There is a subtlety regarding the evolution of the autocorrelation function that must be highlighted. The autocorrelation function by definition is a symmetric function defined for both negative and positive time; however, the GLE Eq. (1) is only defined for positive time and thus the evolution of the autocorrelation function in Eq. (4) is only defined for positive time. This point will be important when considering the FT of the memory kernel in this section.

The first memory kernel can be shown by the second fluctuation dissipation theorem to be the autocorrelation (and thus symmetric) function of the stochastic forcing function

[21]:

$$m_1(t) = \frac{\langle \mathcal{S}(t)\mathcal{S}(0)\rangle}{\langle \mathcal{G}(0)\mathcal{G}(0)\rangle}. \tag{5}$$

Arbitrarily higher-order equations can be constructed by interchanging the positions of the autocorrelation function $m_{n-1}(t)$ with the memory kernel $m_n(t)$ and introducing a new memory kernel $m_{n+1}(t)$ to replace $m_n(t)$ into the convolution term. This is known as the Mori-Zwanzig chain, with the memory kernel autocorrelation functions acting as the links of the chain:

$$\frac{dm_n(t)}{dt} = \lambda_n m_n(t) - \Lambda_n \int_0^t m_{n+1}(t-t')m_n(t')dt' \quad t \geqslant 0. \tag{6}$$

By convention, all of the considered autocorrelation functions are normalized such that $m_n(0) = 1$ [11]. For the first autocorrelation function $[m_0(t)]$ this can be achieved by dividing every term in Eq. (4) by an appropriate normalizing factor. For the remaining memory autocorrelation functions the normalization is ensured by the form of the Λ_n relaxation factors.

In this paper we use the following FT convention:

$$F(\omega) = \mathcal{F}[f(t)](\omega) = \int_{-\infty}^{\infty} f(t)e^{-i\omega t}\,dt \tag{7}$$

$$f(t) = \mathcal{F}^{-1}[F(\omega)](t) = \frac{1}{(2\pi)}\int_{-\infty}^{\infty} F(\omega)e^{i\omega t}\,d\omega. \tag{8}$$

Notice that an equivalent normalization of unity requirement on the FT of the nth memory autocorrelation function, which we refer to as the nth order memory power spectrum, $M_n(\omega)$, can be constructed using the Wiener-Khinchin theorem [22]:

$$\int_{-\infty}^{+\infty} M_n(\omega)d\omega = 2\pi. \tag{9}$$

The form of the λ_n relaxation parameters can be determined from manipulation of Eq. (4) as

$$\lambda_n = \lim_{t\to 0^+}\frac{dm_n(t)}{dt} = 0 \quad \forall \quad m_n(t) \in C^1. \tag{10}$$

Notice that because the time correlation function in Eq. (4) is only defined for positive time, the limit is taken from above. Due to the symmetry of autocorrelation functions, as long as there is no breakdown in smoothness of the derivative (that is it belongs to the C^1 or higher set of functions) at the origin, this parameter must be zero in continuous time. An equivalent requirement can be constructed in the frequency domain:

$$\lambda_n = \lim_{h\to 0^+}\frac{1}{2\pi}\frac{\int_{-\infty}^{\infty} M_n(\omega)(e^{i\omega h}-1)d\omega}{h}. \tag{11}$$

By the dominated convergence theorem, if $P(\omega)$ decays $O(\omega^{-2})$ or faster, the limit can be brought inside the integral and the integrand evaluated to yield the indeterminate function $0/0$. Applying L'Hôpital's rule, if $P(\omega)$ decays $O(\omega^{-3})$ or faster, then the limit can again be brought inside the integral and shown to be zero. Since the power spectrum must be symmetric, this $O(\omega^{-3})$ decay is not possible. Thus, if $P(\omega)$ decays $O(\omega^{-4})$ or faster, λ is zero. As a counter example, an autocorrelation function with a $c(t) = e^{-a|t|}$ and $P(\omega) \equiv O(\omega^{-2})$ structure, which has a nonzero λ value, was considered in Ref. [16].

The Λ_n relaxation parameter cannot be defined from Eq. (4) without the previously stated constraint that $M_{n+1}(0) = 1$. Taking the derivative of Eq. (4), applying the Leibniz rule for differentiating the convolution term, and taking the limit as time goes to zero yields

$$\Lambda_n M_{n+1}(0) = \lambda_n \lim_{t\to 0^+}\frac{m_n(t)}{dt} - \lim_{t\to 0^+}\frac{d^2m_n(t)}{dt^2}. \tag{12}$$

As discussed previously, if $M_n(\omega)$ decays $O(\omega^{-4})$ or faster, λ_n will be zero. Enforcing the condition that the memory kernel $M_{n+1}(t)$ must be unity at time zero gives the following expression:

$$\begin{aligned}\Lambda_n &= -\lim_{t\to 0^+}\frac{d^2m_n(t)}{dt^2}, \quad \forall \quad m_n(t) \in C^1 \\ &= \frac{1}{2\pi}\int_{-\infty}^{+\infty}\omega^2 M_n(\omega)d\omega.\end{aligned} \tag{13}$$

The second expression has been generated by application of the Weiner-Khinchin theorem and is in agreement with that obtained in Refs. [23] (which considered a similar Mori-Zwanzig kinetic equation with λ set to zero) and [18]. Notice that this expression shows that Λ_n is a measure of the spread (second central moment) of the $M_n(\omega)$ memory power spectrum.

III. NON-MARKOV PARAMETERS

The non-Markov parameters $\epsilon_n(\omega)$ are defined as the square root of the ratio of FT of the preceding memory kernel $[M_{n-1}(\omega)]$ and the memory kernel $M_n(\omega)$ [5,11,13]:

$$\epsilon_n(\omega) = \sqrt{\frac{M_{n-1}(\omega)}{M_n(\omega)}} \quad n \geqslant 1. \tag{14}$$

By the Wiener-Khinchin theorem, the $M_0(\omega)$ term in the first NMP is immediately recognized as the measured power spectrum of the signal. The higher-order memory power spectrum can be evaluated by taking the FT of both sides of Eq. (4), with a Heaviside distribution included in the Fourier kernel. The resultant equation in Fourier space can be algebraically rearranged to yield an expression for the FT of the memory kernel. The inclusion of the Heaviside distribution is necessary as the evolution of the autocorrelation function in Eq. (4) is only valid for positive time, whereas the FT is defined for all positive and negative time. This function was evaluated previously in Ref. [16]:

$$M_n(\omega) = \frac{\lambda_{n-1}}{2\Lambda_{n-1}} + \frac{4}{\Lambda_{n-1}}\left(\frac{M_{n-1}(\omega)}{M_{n-1}(\omega)^2 + \mathcal{H}[M(\omega)_{n-1}(\omega)]^2(\omega)}\right). \tag{15}$$

Where $\mathcal{H}[\cdots] =$ is the Hilbert transform integral, which is defined in terms of the Cauchy principal value (p.v.):

$$\mathcal{H}[F(\omega)](\omega) = \frac{1}{\pi}\,\text{p.v.}\int_{-\infty}^{+\infty}\frac{F(\omega')}{\omega-\omega'}\,d\omega'. \tag{16}$$

Note that care must be taken with sampling continuous time systems in order for the discrete time form of the memory kernel to be equivalent to Eq. (15) [17].

The nth memory power spectrum $M_n(\omega)$ can be determined from the previous memory power spectrum. The nth memory power spectrum can then be constructed in a modular fashion from the measured power spectrum $M_0(\omega)$ using Eqs. (10), (13), and (15). For signals with memory kernel spectrums with decay rates $O(\omega^{-4})$ or greater, or equivalently with memory autocorrelation functions belonging to the C^1 or greater set this has a particularly simple form:

$$M_n(\omega) = \frac{4^n M_0(\omega)}{\prod_{i=0}^{n-1} \Lambda_i \{M_i(\omega)^2 + \mathcal{H}[M_i(\omega)]^2(\omega)\}^2}. \quad (17)$$

Thus, the FT of the memory kernels are defined in terms of a product series of nonlinear integral transforms of the measured power spectrum. The generalized NMP is given in closed form using Eqs. (14) and (15):

$$\begin{aligned}\epsilon_n(\omega) &= \frac{\sqrt{\Lambda_{n-1}}}{2}\sqrt{M_{n-1}(\omega)^2 + \mathcal{H}[M_{n-1}(\omega)]^2} \\ &= \frac{\sqrt{\Lambda_{n-1}}|V_{n-1}(\omega)|}{2}, \end{aligned} \quad (18)$$

where $|V_n(\omega)|$ is the amplitude envelope [7] of the memory kernel spectrum. Thus, when the conditions of Eq. (10) are satisfied, the first NMP is solely a function of the spread and amplitude envelope of the power spectrum. The description of the memory power spectrum in Eq. (15) as a ratio of the previous memory power spectrum and its amplitude envelope suggests two interesting properties of these parameters. First, the successive memory power spectra will decay at slower rates than the previous memory power spectra. Second, since the action of the amplitude envelope is to smooth out the underlying function, the higher memory power spectra will become flatter and flatter over the support of the original power spectrum. We will show this behavior of the higher-order memory power spectra in the systems we analyze in Secs. IV and V.

This raises questions about the validity of using the higher-order NMP to analyze a measured system. First, in the noise-free case the successive amplitude envelopes will "smear" out the measured spectrum, thereby losing the correlation structure. Thus, the higher-order NMP may not be measuring anything "interesting" about the system. This interpretation may explain why two of the physical systems considered in Ref. [18] (ideal gas and an ideal gas with linear interaction perturbations) had distinct ZF-NMP$_1$ but identical higher-order zero-frequency NMP values. Second, in any signal acquisition process, noise will certainly be present. It can be seen from Eq. (4), with $\lambda = 0$, that extracting the memory kernel is a deconvolution of a Volterra integral equation of the first kind. These convolution equations are often ill posed [24]. Thus, it is possible that in any measured system, interesting structure seen in the higher-order NMP are actually the manifestation of numerical errors and or noise.

Notice that by the symmetry property of the power spectrum $[M_n(\omega') = M_n(-\omega')]$ the Hilbert transform of the power spectrum is zero at zero frequency:

$$\mathcal{H}[M_n(\omega)](0) = \frac{-1}{\pi}\,\text{p.v.}\int_{-\infty}^{+\infty}\frac{M_n(\omega')}{\omega'}\,d\omega' = 0. \quad (19)$$

Using Eqs. (14), (17), and (19), closed form expressions for the zero-frequency values of the generalized NMP that solely depend on the spread and the DC offset of the nth memory power spectrum can be obtained. These expressions are in agreement with the calculations in Ref. [18]:

$$\epsilon_n(0) = \frac{\sqrt{\Lambda_n}}{2}M_n(0). \quad (20)$$

We pay particular attention to the zero-frequency value of the first NMP (ZF-NMP$_1$):

$$\epsilon_1 = \frac{M_0(0)}{2\sqrt{2\pi}}\sqrt{\int_{-\infty}^{\infty}\omega^2 M_0(\omega)d\omega}. \quad (21)$$

The complicated structure of the Mori-Zwanzig chain Eq. (4) obfuscates the fact that the ZF-NMP$_1$ (and indeed the generalized NMP) is solely a function of the measured power spectrum. Indeed the Mori-Zwanzig equations and associated memory kernels do not even need to explicitly be considered. These results suggest that signal metrics to differentiate complex systems can be developed by analyzing different properties of the measured power spectrum. The previous success of the NMP [5,6,12,13,16] helps elucidate specifically what properties (spectral spread and DC offset) should be explored, but does not necessarily require Mori-Zwanzig theory to interpret the results.

The dependence of the ZF-NMP$_1$ on the DC offset value of the spectrum raises an important digital signal processing issue regarding the use of this parameter for "real-world" measured systems. Spectrum values determined from nonparametric estimation methods (e.g., Welch's method) will be random variables (typically Chi-squared distributed [25]). Thus, if the ZF-NMP$_1$ is to be used as a signal metric, it would be advisable to use a large number of signal samples and appropriate statistical tests or parametric spectrum estimation techniques (e.g., Burg's method) to reduce the variance associated with this metric [25].

It is interesting to note that the rich class of behavior generated by Markovian dynamics will all have a common ZF-NMP$_1$ value of infinity [11]. Thus, in this framework different purely Markov systems cannot be differentiated, representing a degeneracy. Methodologies have been developed to explore and analyze the behavior of these Markov processes given only measurements of the system. An example of this is modeling the unknown Markov system as a set of coupled, Langevein equations (representing the restricted case of Eq. (1) with the memory kernel term set to zero) and performing an Eigenanalysis on the diffusion matrix of the corresponding Fokker-Planck equation [26]. This approach was used to successfully model the power response curves of wind farm turbines [27].

IV. EXPLICIT CALCULATION OF ZF-NMP$_1$ FOR PHYSICAL SYSTEMS

In this section we derive the ZF-NMP$_1$ for three instructive stochastic processes: simple harmonic oscillation driven by white noise, band-limited white noise, and the output of white noise passed through an idealized all-pole filter. We perform this analysis to understand how sensitive this parameter is to specific variation in the measured power spectra. This provides insight into what changes, in terms of spectral properties, the ZF-NMP$_1$ was detecting in the measured complex systems analyzed in [5,12,14,15].

A. Simple harmonic oscillation driven by white noise

The SHO driven by white noise provides an excellent bridge between understanding the (ZF-NMP$_1$) in the original framework of the Markovity of the system and the signal processing framework of the structure of the spectrum. This system also provides one of the few systems where the higher-order memory power spectra can be analytically calculated. The difficulty in the general case is due to the evaluation of the Hilbert transforms. The dynamics of the SHO driven by white noise are given by

$$\frac{d^2x(t)}{dt^2} + 2\zeta\omega_0\frac{dx(t)}{dt} + \omega_0^2 x(t) = W(t), \tag{22}$$

where ω_0 is the angular natural frequency, ζ is the damping ratio, and $W(t)$ is the white noise stochastic process with constant amplitude power spectrum.

The normalized power spectrum of this process is given by [28]

$$M_0(\omega) = \frac{4\zeta\omega_0^3}{\left(\omega_0^2 - \omega^2\right)^2 + 4\zeta^2\omega_0^2\omega^2}. \tag{23}$$

Notice that $M_0(\omega)$ decays $O(\omega^{-4})$ and thus $\lambda_0 = 0$. The contour integrals required to determine the Λ_0 from the spectral form of Eq. (13) are relatively difficult for arbitrary ζ, ω_0 parameters. Instead, the Λ_0 relaxation parameter will be determined from the autocorrelation function form for the different damping regimes: over, under, and critically damped.

The normalized autocorrelation structure of the under-damped (UD) SHO is given by [29]

$$m_0(t)_{\mathrm{UD}} = e^{-\zeta\omega_0|t|}\left[\cos(\omega_1 t) + \frac{\zeta}{\sqrt{1-\zeta^2}}\sin(\omega_1|t|)\right], \tag{24}$$

where $\omega_1^2 = \omega_0^2(1-\zeta^2)$ is the damped natural frequency. The critically damped case is determined in the limit of $\omega_1 \to 0$. The overdamped case is determined by setting $\omega_1 \to i\omega_1$, which transforms the trigonometric functions in Eq. (24) to hyperbolic trigonometric functions.

The Λ_0 relaxation parameter is given for all three damping regimes by

$$\Lambda_0 = \omega_0^2. \tag{25}$$

The ZF-NMP$_1$ of the SHO driven by white noise can now be written using Eqs. (20), (23), and (25) as

$$\epsilon_1(0) = 2\zeta. \tag{26}$$

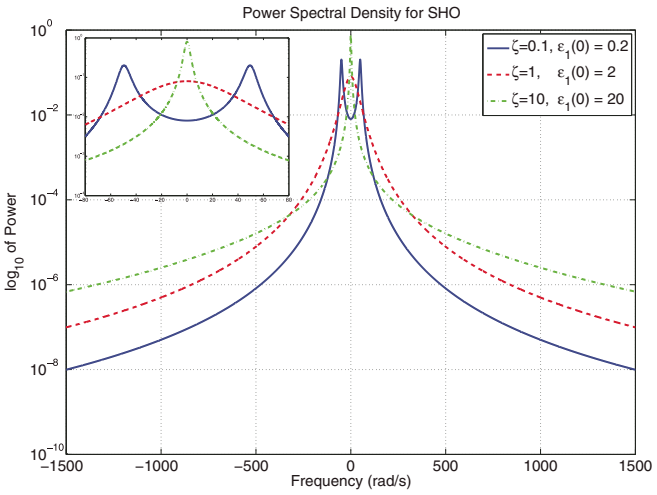

FIG. 1. (Color online) Power spectral density $[M_0(\omega)]$ for the SHO for different damping regimes of under ($\zeta = 0.1$), over ($\zeta = 10$), and critically damped ($\zeta = 1$). Notice that as the damping ratio is increased the spectrum becomes more spread, the zero-frequency power increases, and the NMP increases. Inset is the low-frequency behavior of the three oscillators.

Notice that the ZF-NMP$_1$ depends solely on the damping ratio, which is a measure of the amount of energy dissipation in the system. Inspection of Fig. 1 shows that as the damping ratio is increased the measured spectrum $M_0(\omega)$ becomes more spread out and the DC offset increases. The sole dependence of the ZF-NMP$_1$ on this ratio is particularly interesting, because it explicitly states that the "Markovity" of this system (as measured by the ZF-NMP$_1$) is directly related to how quickly the energy is dissipated. If the system is under-damped then the deterministic free response will dominate the stochastic forcing by the white noise process. If the system is over-damped then the predictable free response will quickly die out and the response will be dominated by the stochastic white noise process. Thus, the damping is a measure of the memory of the system. This analysis is entirely consistent with the original description of the ZF-NMP$_1$ [6] in terms of the Markovity of a system with respect to its environment.

Notice that in the limit of an infinitely large damping ratio the NMP approaches infinity. Analyzing the SHO dynamics in the limit of the β term approaching infinity and recognizing that the white noise process can informally be written as the time derivative of a Wiener process, $W(t) = dw(t)/dt$, the dynamics of this system in this limit can be written as

$$dx(t) = -\frac{\omega_0}{2\zeta}x(t)dt + \frac{1}{2m\zeta\omega_0}dw(t). \tag{27}$$

This is the stochastic differential equation, which describes the Ornstein-Uhlenbeck process. It is interesting to note that this is a process that satisfies the conditions of being stationary, Markov and Gaussian [30]. Thus, the NMP of the Ornstein-Uhlenbeck process is infinite, which is in agreement with the original definition of this parameter.

The higher-order memory power spectrum and kernel for the critically damped SHO (the Hilbert transform being too

difficult for arbitrary damping ratios) can be analytically calculated:

$$|V_0(\omega)|^2 = \frac{4\left(\omega^2 + 4\omega_0^2\right)}{\left(\omega^2 + \omega_0^2\right)^2}$$

$$M_1(\omega) = \frac{4\omega_0}{\omega^2 + 4\omega_0^2} \tag{28}$$

$$m_1(t) = e^{-2\omega_0 t}. \tag{29}$$

Notice that $M_1(\omega)$ decays $O(\omega^{-2})$ and thus λ will be nonzero. Using Eqs. (10), (12), and (29),

$$|V_1(\omega)|^2 = \frac{4}{\omega^2 + 4\omega_0^2}$$

$$\frac{M_1(\omega)}{|V_1(\omega)|^2} = \omega_0 \tag{30}$$

$$\lambda_1 = -2\omega_0 \tag{31}$$

$$\Lambda_1 = 0. \tag{32}$$

Thus, the $M_2(\omega)$ memory power spectrum will be infinite due to the scaling by the inverse of Λ_1. This shows that the second-order zero frequency NMP will be zero. Analysis of Eq. (15) shows the higher-order memory kernels and generalized NMP will give pathological divide by zero solutions. This result can be explained as follows: The exponential first-order memory function satisfies the differential equation:

$$\frac{dm_1(t)}{dt} = \lambda_1 m_1(t). \tag{33}$$

This is exactly the Zwanzig-Mori Eq. (6) for the first memory kernel $m_1(t)$ with the convolution term (and thus Λ_1) equal to zero. It is interesting to identify the unscaled second memory power spectrum $M_2(\omega)$ given by Eqs. (30) and (31) [that is not obeying the constraint in Eq. (9)] is white noise. This indicates the second-order memory kernel $m_2(t)$ will be a Dirac δ distribution centered at time zero. This distribution cannot be scaled such that it satisfies the requirements of Eq. (9), which also helps explain why Λ_1 is zero.

Figure 2 shows the first three numerically determined memory kernels for the underdamped harmonic oscillator ($\zeta = 0.25$, $\omega_0 = 200$) using Eqs. (13) and (15) and assuming Eq. (10) is satisfied. Notice that the $M_2(\omega)$ term is constructed assuming $\lambda_2 = 0$ [thus, Λ_2 is defined from Eq. (13) rather than Eq. (12)], so that the flat white noise structure can be identified. Notice that this flattening of the higher-memory kernels is exactly as was postulated in Sec. II.

B. Band-limited white noise

The normalized power spectrum for the white noise process banded between $(-w_0, +w_0)$ is given by

$$M_0(\omega) = \frac{\pi}{\omega_0}[\theta(\omega + \omega_0) - \theta(\omega - \omega_0)], \tag{34}$$

where $\theta(\cdots)$ is the Heaviside distribution. The Λ_0 relaxation parameter is given by the spectral form of Eqs. (13)

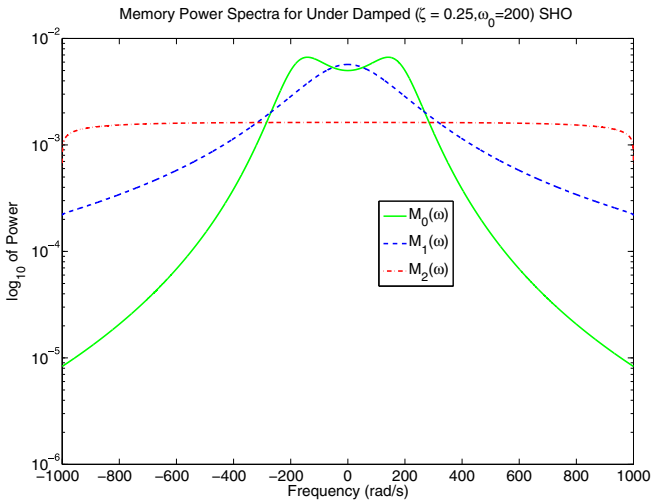

FIG. 2. (Color online) Numerically determined first three memory power spectra for the underdamped SHO. Notice that for the successively higher-memory power spectra the correlation structure is lost, the spectra become more flat, and the third-order memory power spectra $M_2(\omega)$ appear to be approaching a white noise solution. The edge effects are numerical issues associated with the numerical estimate of the Hilbert transform.

and (34):

$$\Lambda_0 = \frac{1}{2\omega_0}\int_{-\omega_0}^{+\omega_0} \omega^2 d\omega = \frac{\omega_0^2}{3}. \tag{35}$$

The first memory power spectrum is given by

$$M_1(\omega) = \frac{12\pi[\theta(\omega + \omega_0) - \theta(\omega - \omega_0)]}{\omega_0\left[\pi^2 + \ln\left(\left|\frac{\omega+\omega_0}{\omega-\omega_0}\right|\right)^2\right]}. \tag{36}$$

The ZF-NMP$_1$ is given by Eqs. (20), (34), and (35):

$$\epsilon_1(0) = \frac{\pi}{2\sqrt{3}}. \tag{37}$$

This is interesting because it shows that the ZF-NMP$_1$ is independent of the bandwidth of the band-limited white noise. Mathematically this can be understood to be due to the normalization requirement, as the noise process occupies more bandwidth and the spread increases, the amplitude of this noise decreases and so does the DC offset. These two parameters must change such that the ZF-NMP$_1$ remains constant. We cannot extend our analysis to the infinite bandwidth white noise process because the correlation structure is a Dirac δ distribution for which it is not possible to normalize to unity, nor define its derivatives in the limit of zero time as is required for the relaxation parameters.

Figure 3 plots the first five numerically determined memory power spectra of the band-limited white noise ($\omega_0 = 50$) system using Eqs. (13), (17), and (34). Notice that all the memory power spectra [except for the measured power spectrum $M_0(\omega)$] converge to a common spectral structure, indicating limited utility of the higher-order NMP. The higher-order Λ_n relaxation parameters will not equal zero because the compact support of the band-limited white noise prevent the memory power spectra from becoming white noise

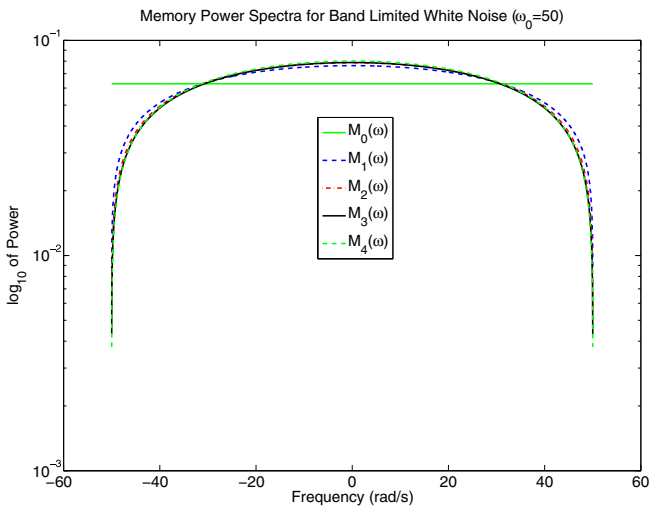

FIG. 3. (Color online) Numerically determined first five memory power spectra for the band-limited white noise case ($\omega_0 = 50$). Notice that the higher-order memory power spectra after the zeroth $M_0(\omega)$ term appear to converge to a common spectral structure.

solutions, or equivalently the autocorrelation function from ever becoming a Dirac δ distribution.

C. Ideal all-pole filter

The ideal all-pole filter refers to a piecewise continuous spectrum that consists in log-log (base e) space of a straight line of height h, which goes from 0 to the corner frequency ω_c, and then another straight line that has a negative slope proportional to the order of m, which goes from the corner frequency ω_c to infinity. The Bode plot of this spectrum is shown in Fig. 4. The actual value of the height h is determined by the normalization requirement of Eq. (9). This is an idealized filter because the cusp (breakdown of the first derivative) at the corner frequency creates an unphysical "infinite-power" requirement on the filter [7]. Intuitively we expect the NMP to depend on both the order

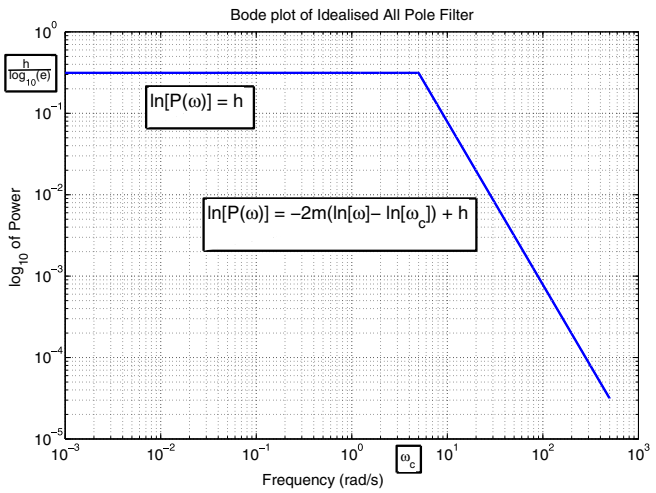

FIG. 4. (Color online) Bode plot of the ideal all-pole filter spectrum with corner frequency ω_c and filter order m.

and corner frequency of the filter, but we show that it depends solely on the slope of the tail (i.e., m) of the power spectrum.

We can mathematically represent the power spectrum of our idealized all-pole filter in log-log (base e) frequency space as

$$\ln[M_n(\omega)] = \begin{cases} h & 0 \geqslant \ln[\omega] \geqslant \ln[\omega_c] \\ -2m\left(\ln\left[\frac{\omega}{\omega_c}\right]\right) + h & \ln[\omega_c] \geqslant \ln[\omega] \geqslant \infty. \end{cases} \tag{38}$$

We can map this to frequency space by taking the antilog (in base e) of both sides of Eq. (38). There are two things to notice: First, the power spectrum is symmetric about the origin, whereas the log-log (in base e) power spectrum is one sided. Thus, we make the solution obtained in frequency space symmetric about the zero-frequency origin. The log-log (in base e) power spectrum when mapped to the power spectrum will start at $\omega = 1$ (because $e^0 = 1$ in the bounds for the constant straight line). We simply extend the bounds of the power spectrum to $\omega = 0$ in frequency space.

The constant $\alpha = e^h$ will be determined such that the power spectrum has the appropriate normalization required by Eq. (9):

$$\alpha = \frac{\pi\,(2m-1)}{2m\omega_c}. \tag{39}$$

The power spectrum is given by

$$M_0(\omega) = \begin{cases} \frac{\pi(2m-1)}{2m\omega_c} & 0 \geqslant |\omega| \geqslant \omega_c \\ \frac{\pi(2m-1)}{2m\omega_c}\left(\frac{\omega}{\omega_c}\right)^{-2m} & \omega_c \geqslant |\omega| \geqslant \infty. \end{cases} \tag{40}$$

In order to simplify analysis, we will only consider ideal all-pole filters of order m of 2 or higher.

The Λ_0 relaxation parameter can be determined from the spectral form of Eqs. (13) and (40):

$$\Lambda_0 = \frac{(2m-1)\,\omega_c^2}{3\,(2m-3)}. \tag{41}$$

Using Eqs. (20), (40), and (41), the ZF-NMP$_1$ is given by

$$\epsilon_1(0) = \frac{\pi}{m}\sqrt{\frac{(2m-1)^3}{48\,(2m-3)}}. \tag{42}$$

The most interesting result from Eq. (42) is that, similar to the band-limited white noise case, the ZF-NMP$_1$ for the ideal all-pass filter is independent of the corner frequency. The ZF-NMP$_1$ is sensitive to the order of the filter. Figure 5 shows an inverse relationship between the decay rate of the tail of the power spectrum and the ZF-NMP$_1$ value. Similar to the SHO, the more spread out the power spectrum, the larger the ZF-NMP$_1$. An obvious difference between these two systems is that the ZF-NMP$_1$ for the SHO is unbounded, whereas (at least for $m \geqslant 2$) the ZF-NMP$_1$ of the ideal all-pole filter is approximately bounded between 1.17 (m = 2) and 0.9 ($m \to \infty$). Notice that while the ZF-NMP$_1$ does depend on the tail of this spectrum, it is not particularly sensitive to it.

It can be seen that the ZF-NMP$_1$ value for the ideal all-pole filter converges to the band-limited white noise case for sufficiently large slope order ($m \approx 10$ or higher). This result is to be expected, because as the slope of the ideal all-pole filter

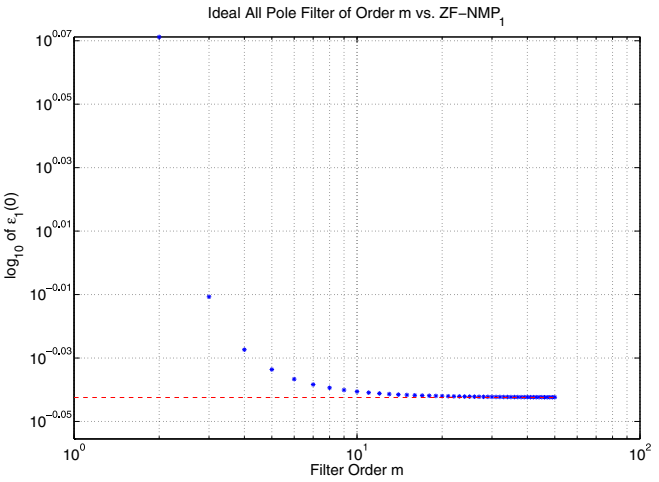

FIG. 5. (Color online) Plot of ZF-NMP$_1$ of the output of white noise fed into the ideal all pole filter vs. slope order (m). Notice that for sufficiently large slope order the NMP converges to the band-limited white noise solution.)

increases, the spectrum will converge to the band-limited white noise spectrum. It is trivial to formally show that the NMP of this idealized all-pole filter converges to the band-limited white noise process in the limit of infinite filter order:

$$\lim_{m\to\infty} \epsilon_1(0) = \lim_{m\to\infty} \pi\sqrt{\frac{(2m)^3}{48m^2\,(2m)}} = \frac{\pi}{2\sqrt{3}}. \qquad (43)$$

Figure 6 plots the first five numerically determined memory power spectra of the ideal all-pole filter ($m = 4$, $\omega_0 = 50$) using Eqs. (13), (17), and (40). Notice that (similar to the critically damped simple harmonic oscillator shown in Fig. 2) the higher-order memory power spectra are flatter and lose the correlation structure present in the measured $M_0(\omega)$ spectrum. This further validates the flattening of the higher memory kernels as postulated previously in Sec. II. Again, this raises questions about the utility of the higher-order NMP as system metrics.

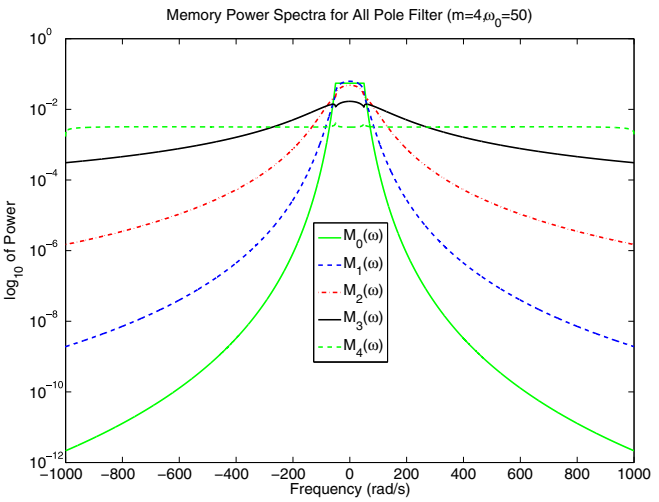

FIG. 6. (Color online) Numerically determined memory power spectra for the ideal all-pole filter ($m = 4$, $\omega_0 = 50$). Notice that the higher-order memory power spectra get considerably flatter.

V. NUMERICAL DETERMINATION OF NMP FROM SAMPLED TIME SERIES

We finish by determining the memory power spectra and ZF-NMP$_1$, using the closed form Eqs. (17)–(20), from what can be considered as a model of the sampled time series of the displacement of the SHO driven by white noise. We model the system as a second-order auto regressive [AR(2)] process:

$$x[n] = \phi_1 x[n-1] + \phi_2 x[n-2] + \epsilon_n,$$
$$\text{where} \quad (\phi_1 = 0.9, \phi_2 = -0.8), \quad \epsilon_n \sim \mathcal{N}(0,1). \qquad (44)$$

The choice of AR coefficients in Eq. (44) can be considered related to the under-damped SHO driven by white noise [31]. We simulate 1000 data points of this process to generate a discrete time series. We determine the memory power spectra and ZF-NMP$_1$ using solely this time series with no *a priori* information about the AR coefficients or innovations, ϵ_n, which define the process. A realization of this process (and thus time series to be analyzed) is shown in Fig. 7.

The power spectrum of this process is determined from the time series using the ARMAsel parametric spectrum estimator. The technical details of this estimator are provided in Ref. [32] but as an overview it fits the data to an optimal order (p) auto regressive, order (q) moving average, or order (r, r-1) auto regressive moving average model determined by an information criteria. This criteria effectively provides a balance between rewarding the reduction in residual variance and punishing the increase in model order complexity. The parametric model that gives the smallest estimate of the prediction error is then selected and the estimated power spectrum is calculated using the fast Fourier transform. Once the power spectrum estimate is obtained, the higher-order memory power spectra and generalized NMP can be determined using Eqs. (13), (17),

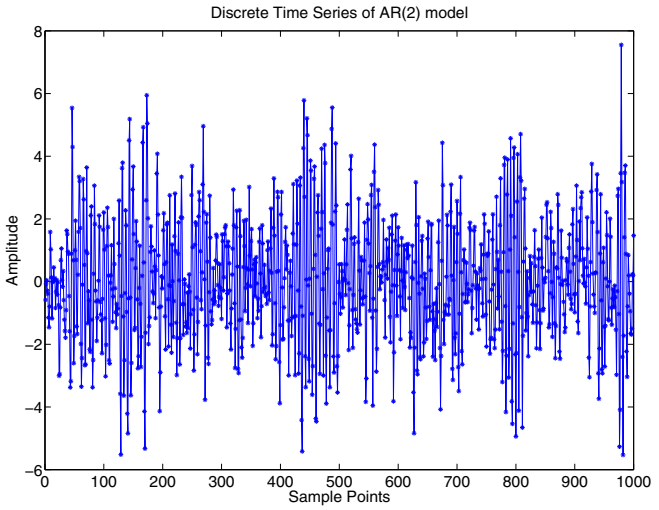

FIG. 7. (Color online) Sample path realization of the AR(2) process [$\phi_1 = 0.9, \phi_2 = -0.8, \epsilon_n \sim \mathcal{N}(0,1)$] generated from Eq. (44). This discrete time series is used to generate the memory power spectra.

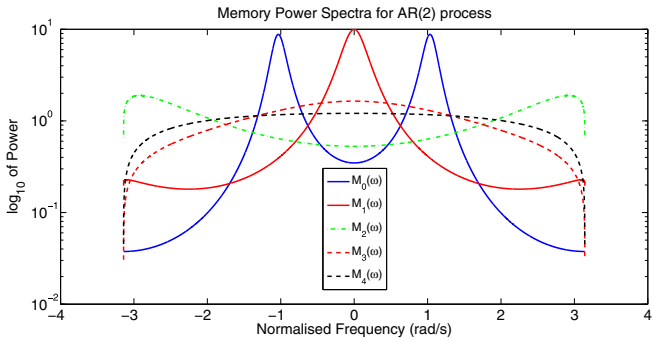

FIG. 8. (Color online) First five numerical memory power spectra estimates of the AR(2) process defined in Eq. (44). Notice that for the successively higher-order memory power spectra the correlation structure observable in the power spectral density is smeared out. Also notice the spectrum is defined over the normalised frequency range of $(-\pi,\pi)$.

and (18). The estimated memory power spectra are shown in Fig. 8. Notice that similar to systems with a continuous power spectrum analyzed in Sec. IV, the higher-order memory power spectra appear to smear out the correlation structure observable in the power spectrum.

An estimate of the ZF-NMP$_1$ of this AR process can be obtained from the time series by estimating the power spectrum with the ARMAsel algorithm and using Eqs. (13) and (20). This estimate (mean $\pm$ standard error) is averaged over 20 realizations (each 1000 data points) of the AR process to give

$$\hat{\epsilon}_1(0) = 0.368 \pm 0.0119. \tag{45}$$

This solution can be compared to the true ZF-NMP$_1$. The unnormalized power spectrum of this process is given by [33]

$$M_0(\omega) = \frac{\sigma^2}{1+\phi_1^2+\phi_2^2-2\phi_1(1-\phi_2)cos(\omega)-2\phi_2 cos(2\omega)}, \tag{46}$$

where σ^2 is the variance of the innovations. Using Eqs. (13), (20), and (46) the ZF-NMP$_1$ of this process can be calculated by numerical integration to be

$$\epsilon_1(0) = 0.359. \tag{47}$$

Therefore, it can be seen that with appropriate statistical averages (which are necessary given finite-time recordings of stochastic processes) the ZF-NMP$_1$ can be accurately estimated from the time series data alone.

This example highlights several key points that are not immediately clear in the analysis of the physically motivated systems considered in Sec. IV. First, this time series could be acquired without any knowledge of the underlying physics driving this system. This would make the Mori-Zwanzig interpretation of the non-Markovity (which requires partitioning the dynamical system into subsets of observables of interest and an interacting environment) extremely difficult to perform. This is in contrast to the signal processing approach introduced in this paper which interprets the non-Markovity spectrum in the concrete terms of operations on the measured power spectra. Second, this example provides a "real world" application of estimating the non-Markovity spectra where the underlying continuous power spectra is unknown and only discrete samples of the measured time series corrupted with noise are available. Problems of this nature are commonplace in signals analysis and thus it is important to identify that the closed form Eqs. (17) and (18) for the memory power spectra and generalized NMP are applicable to this class of problem. We refer the reader to Ref. [17] for a detailed description regarding the issues associated with interpreting the underlying continuous memory kernel from its discrete time estimate.

VI. CONCLUSIONS

The generalized non-Markov parameters have been used to successfully differentiate states (as defined by the degree of chaosisity and randomness) of complex interacting systems. In this paper we have shown these parameters can be understood as a set of closed-form expressions that only depend on a nonlinear set of integral transform operations on the measured signal's power spectrum. We have argued that the operations yielding the higher-order memory power spectra and generalized NMP veil the underlying correlation structure of the measured system in agreement with Ref. [17]. We have supported this argument with numerical simulation of four instructive stochastic processes: a SHO driven by white noise, band-limited white noise, the output of white noise fed into an ideal all pole filter and an AR(2) process with Gaussian innovations. These results suggest a sensitivity of the ZF-NMP$_1$ to the decay rate of the tail of the spectrum.

Last, we have shown that under the appropriate condition of C^1 or higher smoothness of the autocorrelation [or equivalently $O(\omega^{-4})$ or faster decay rates of the tail of the spectral function], the closed form expression for the ZF-NMP$_1$ can be reduced to depending solely on the spread and DC offset of the measured power spectrum. These results provide an alternative interpretation of the generalized NMP, which only depends on the measured signal and does not require knowledge of Mori-Zwanzig theory, nor interpretation of a complex relationship between a measured system and its environment. We have shown that these equations for the memory power spectra and generalized NMP can readily be applied to systems where only noisy discrete time samples are available. These simplified expressions of the NMP in light of its previous success in the analysis of complex systems provides insight into what properties of the spectrum could be used in future signal analysis of complex systems.

[1] K. Bassler, G. Gunaratne, and J. McCauley, Physica A **369**, 343 (2006).

[2] D. T. Schmitt and M. Schulz, Phys. Rev. E **73**, 056204 (2006).

[3] C. Chen, Y. Hsu, H. Chan, S. Chiou, P. Tu, S. Lee, C. Tsai, C. Lu, and P. Brown, Exp. Neurol. **224**, 234 (2010).

[4] A. Knežević and M. Martinis, Int. J. Bifurcation Chaos **16**, 2103 (2006).
[5] R. Yulmetyev, P. Hänggi, and F. Gafarov, Phys. Rev. E **65**, 046107 (2002).
[6] R. Yulmetyev, P. Hänggi, and F. Gafarov, J. Exp. Theor. Phys. **96**, 572 (2003).
[7] A. Carlson and P. Crilly, *Communication Systems: An Introduction to Signals and Noise in Electrical Communication* (McGraw Hill, New York, 2010).
[8] M. Baptista, E. Ngamga, P. Pinto, B. Margarida, and J. Kurths, Phys. Lett. A **374**, 1135 (2010).
[9] J. P. Crutchfield and K. Young, Phys. Rev. Lett. **63**, 105 (1989).
[10] D. Feldman and J. Crutchfield, Phys. Lett. A **238**, 244 (1998).
[11] R. Yulmetyev, P. Hänggi, and F. Gafarov, Phys. Rev. E **62**, 6178 (2000).
[12] R. Yulmetyev, F. Gafarov, P. Hänggi, R. Nigmatullin, and S. Kayumov, Phys. Rev. E **64**(6), 066132 (2001).
[13] R. Yulmetyev, S. Demin, R. Khusnutdinov, O. Panischev, and P. Hänggi, Nonlin. Phenom. Complex Syst. **9**, 313 (2007).
[14] R. Yulmetyev, S. Demin, R. Khusnutdinov, O. Panischev, and P. Hänggi, Nonlin. Phenom. Complex Syst. **94**, 313 (2006).
[15] R. Yulmetyev, S. Demin, O. Y. Panischev, P. Hänggi, S. Timashev, and G. Vstovsky, Physica A **369**, 655 (2006).
[16] J. J. Varghese, K. J. Weegink, P. A. Bellette, T. Coyne, P. A. Silburn, and P. A. Meehan, in *Proceedings of the 33rd Annual International Conference of the IEEE EMBS, Boston, MA, August 30–September 3* (IEEE, Piscataway, NJ, 2011), pp. 2707–2711.
[17] M. Niemann, T. Laubrich, E. Olbrich, and H. Kantz, Phys. Rev. E **77**, 011117 (2008).
[18] R. Yulmetyev and N. Khushnutdinov, J. Phys. A **27**, 5363 (1994).
[19] P. Hänggi, Z. Phys. B **314**, 407 (1978).
[20] R. Zwanzig, *Nonequilib. Stat. Mech.* (Oxford University Press, Oxford, 2001).
[21] G. Mazenko, *Nonequilib. Stat. Mech.* (WILEY-VCH Verlag GmbH & Co. KGaA, Weinhelm, Germany, 2006).
[22] R. N. Bracewell, *The Fourier Transform and Its Applications* (Mcgraw-Hill, New York, 2000).
[23] R. Yulmetyev, R. Galeev, and V. Shurygin, Phys. Lett. A **4**, 258 (1996).
[24] P. Hansen, Numer. Alg. **29**, 323 (2002).
[25] D. Percival and A. Walden, *Spectral Analysis for Physical Applications: Multitaper and Conventional Univariate Techniques* (Cambridge University Press, Cambridge, 1993).
[26] V. V. Vasconcelos, F. Raischel, M. Haase, J. Peinke, M. Wächter, P. G. Lind, and D. Kleinhans, Phys. Rev. E. **84**, 031103 (2011).
[27] F. Raischel, T. Scholz, V. V. Lopes, and P. G. Lind, Phys. Rev. E **88**, 042146 (2013).
[28] W. Coffey, Y. Kalmykov, and J. Waldron, *The Langevin Equation With Applications in Physics, Chemistry and Electrical Engineering* (World Scientific, Singapore, 1996).
[29] M. Wang and G. Uhlenbeck, Rev. Mod. Phys. **17**, 323 (1945).
[30] J. Doob, Ann. Math. **43**, 351 (1942).
[31] L. Lankhorst, J. Atmos. Oceanic Technol. **23**, 1583 (2006).
[32] P. Broersen, IEEE Trans. Instrum. Meas. **49**, 766 (2000).
[33] D. Wilks, *Statistical Methods in the Atmospheric Sciences*, Vol. 100(3) (Elsevier, New York, 2011).